WIND TUNNEL INVESTIGATION OF FLOWFIELD ON THE FOWLER FLAP AND IN THE COVE USING PIV METHOD

Marian Zabloudil*, Zdeněk Pátek*, Petr Vrchota*
***VZLÚ - Aeronautical research and Test Institute, Prague, Czech Republic**

Keywords: *PIV, airfoil, Fowler flap, cove,*

Abstract

An experimental and CFD investigation was conducted to study the influence of the Fowler flap cove geometry on the flowfield in the flap slot. The airfoil for which the study was made was a modified NASA LS(1) series airfoil. The flowfield was experimentally studied in a low-speed wind tunnel using PIV method. Results of the wind tunnel experiments were compared with the CFD results. Different cove geometries were studied mainly with focus to evaluate the influence of the open gap in the cove. It was observed, that the overall aerodynamic characteristics changed only slightly.
The comparison with CFD results confirmed the findings made by the experimental measurements and flowfield visualization.

1 Introduction

Extensive effort has been devoted to study the multielement airfoils including airfoils with Fowler flaps, very frequent due to their high efficiency. The research has been mostly focused on the global aerodynamic performance, the work focused on the flowfield has typically studied the global situation over the multielement airfoil. The studies of details of the flowfield in the cove between the main element and the flap mostly addressed the pressure on the surfaces and/or velocity distribution in the fresh flow in the slot (for example [1] to [5]). The vortex at trailing side of the main element, which is extremely important as is contributing to form the effective shape of the slot, has not attracted much attention in detailed experimental testing. CFD studies show the vortex but experimental results in the form of the visualization of the vortex and/or in the form of the velocity field directly in the cove vortex seem to be extremely rare.

This study presents experimental research of the cove vortex for the essentially different shapes of cove using PIV (Particle Image Velocimetry) technique, and compares the experimental results with CFD results. CFD results also support better understanding of the phenomena as, in the second stage, the computation boundary conditions were modified according to experimental results and thus additional data, not contained in experimental results, were obtained.

2 Symbols

c	airfoil chord
c_D	drag coefficient
c_L	lift coefficient
c_m	moment coefficient
α	angle of attack
δ	flap deflection

3 Experimental Setup

3.1 Airfoil Model

A low-speed airfoil section suitable for general aviation use was examined. The airfoil is a modification of the NASA LS(1) airfoils series. The maximum thickness is of 16 percent of the airfoil chord. The Fowler flap chord is of 30 percent of the total airfoil chord (see Fig. 1).

Fig.1. The Airfoil with the Fowler Flap

Two different shapes of the trailing part of the main airfoil were tested (see Fig. 2):

- smoothly shaped with sharp bottom edge overlapping the bottom leading edge of the retracted flap
- unshaped open gap behind the rear wing spar

The wind tunnel model, depicted in Fig 1, was in the form of a rectangular wing with circular endplates. The span was 1.2 m and the chord 0.6 m.

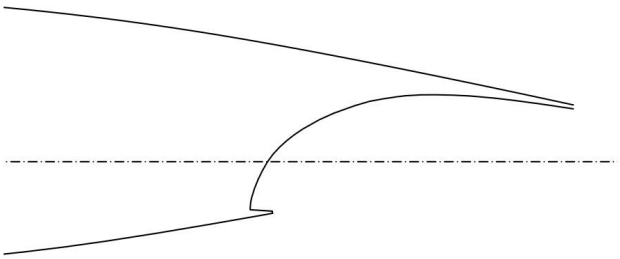

Fig. 2. Smoothly Shaped Trailing Part of the Airfoil

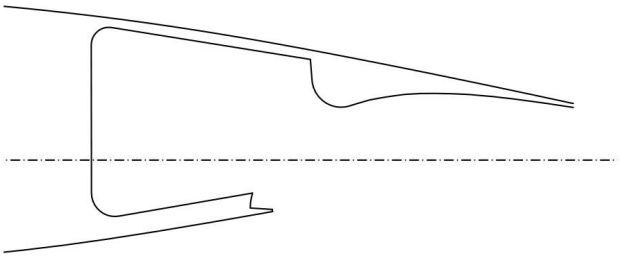

Fig. 3. Unshaped Trailing Part of the Airfoil

3.2 Studied Configurations

Two configurations were studied for both geometries. The Take-off configuration, with flap deflection of 20 degrees, vertical gap between the trailing part of the main airfoil 3 percent of *c* and horizontal overlap 2 percent of *c*. And the Landing configuration, with flap deflection of 35 degrees, vertical gap between the trailing part of the main airfoil 3 percent of *c* and horizontal overlap 0 percent of *c*.

3.3 Wind Tunnel

The tests were performed in the 3m LSWT low speed wind tunnel at VZLU - Aeronautical Research and Test Institute in Prague. The wind tunnel used was an atmospheric type with open test section of 3 meters diameter. The model was suspended on a mechanical balance to measure lift, drag and pitching moment.

3.4 PIV Device

The PIV system consisted of the laser with wave length 527 nm and power 20 mJ per pulse, camera with resolution 1,2 Mpx, maximum speed 1024 fps in full resolution.

Settings of the PIV system was: the camera resolution 1280 x 1024 px, extension tubes with 8 mm length for the mount of the lens with 50 mm focal length were used. The speed was 1000 fps and time between pulses 100 microseconds.

The size of the investigated area was 84 mm x 63 mm (see Fig. 4).

The laser sheet was in the plane parallel to the free stream and the exposured area was between the airfoil and the flap. The camera was placed on the model side and scanned the exposured area through the window in the endplate.

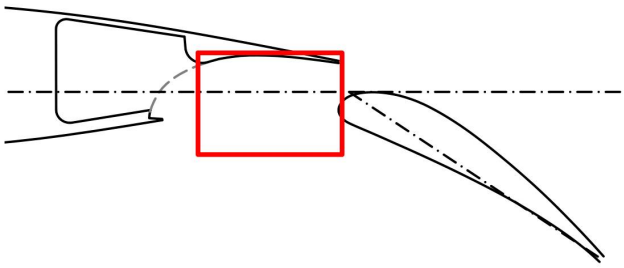

Fig. 4. The Area of PIV Visualization

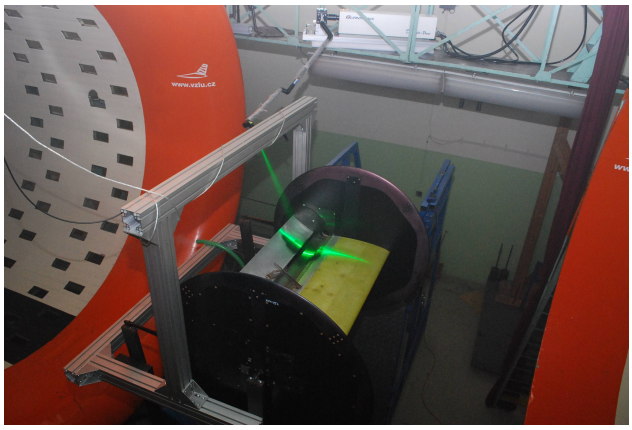

Fig. 5. The Airfoil Model in the Wind Tunnel

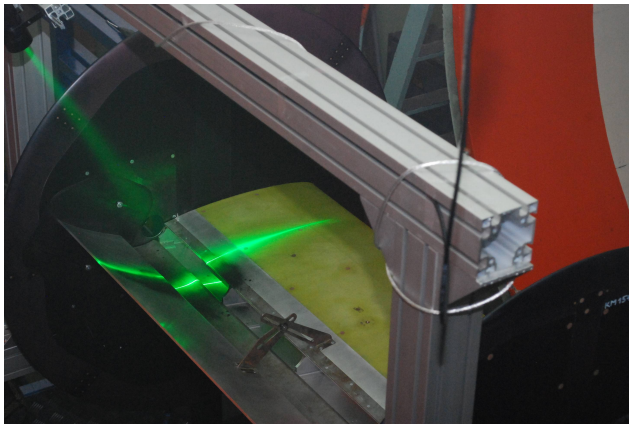

Fig. 6. Detail of the Laser Sheet

4 Experimental Results

All tests were performed at the Reynolds number $2.1 \cdot 10^6$ and Mach number 0.15. The data were processed with all standard wind tunnel corrections for airfoil testing applied. The uncertainties of c_L were ± 0.01, of c_D ± 0.001 and of c_m ± 0.001.

The wind tunnel measurements showed just slight differences in the overall aerodynamic characteristics of the two geometries. The most significant difference was the maximum lift coefficient and also little higher drag of the unshaped geometry [6].

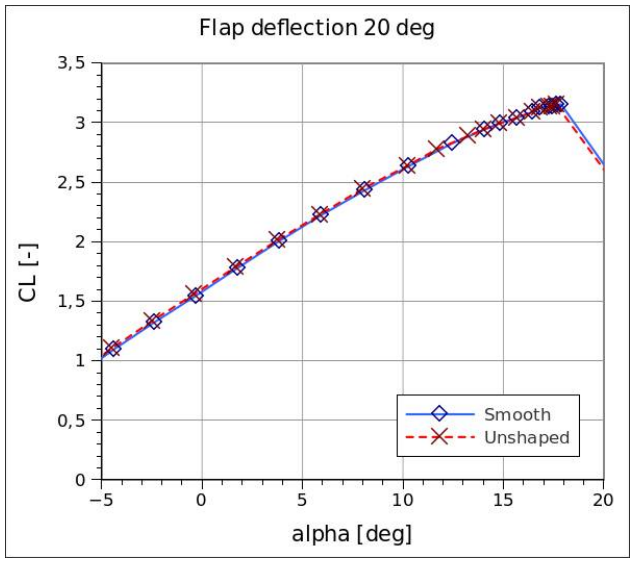

Fig. 7. Lift Curves for Take-off Configuration (Wind Tunnel Results)

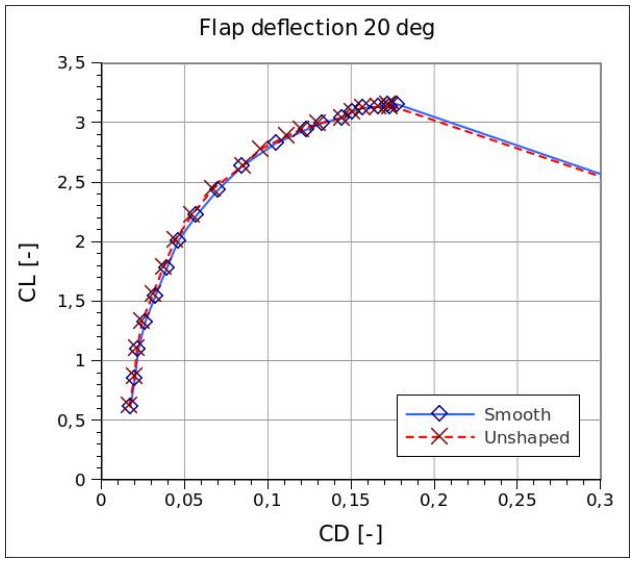

Fig. 8 Polar Curves for Take-off Configuration (Wind Tunnel Results)

The PIV visualization showed, that there is a vortex in the airfoil cove, which creates a new efficient geometry of the airfoil which determines the path of the passing stream. This vortex seems to have approximately the same size for both geometries, which explains similar global aerodynamic characteristics (see Fig. 9. to Fig. 12.).

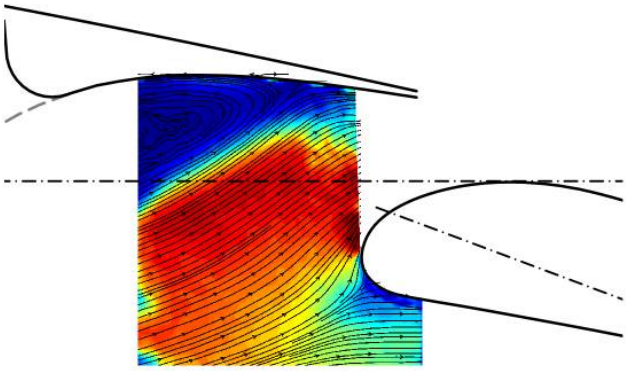

Fig. 9. Smooth geometry, Take-off configuration, alpha 10 deg

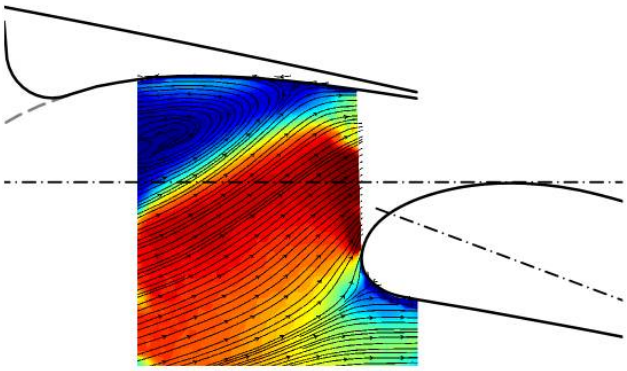

Fig. 10. Unshaped geometry, Take-off configuration, alpha 10 deg

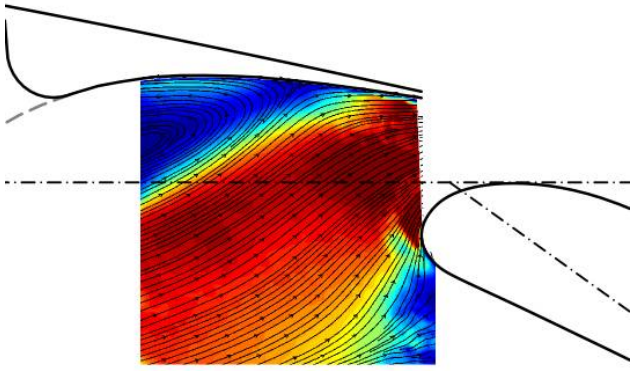

Fig. 11. Smooth geometry, Landing configuration, alpha 10 deg

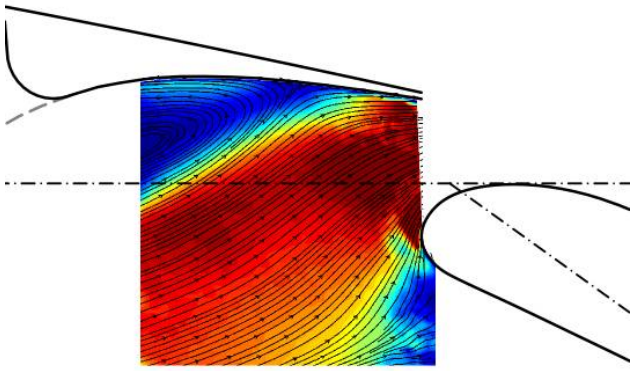

Fig. 11. Unshaped geometry, Landing configuration, alpha 10 deg

5 CFD Method

STAR-CCM+ complex CFD software environment was used for the grid generation and the CFD calculations. It uses finite volume method to solve governing equations on unstructured grids.

The grid was created by hexahedral elements with prismatic boundary layer. The number of cells was approximately 50 000.

Full RANS mode with two equations model of turbulence k-ω SST was used.

6 CFD Results

The CFD results did not show any significant difference of integral aerodynamic characteristics for the studied cases (see Fig. to Fig. 13. and Fig. 14.).

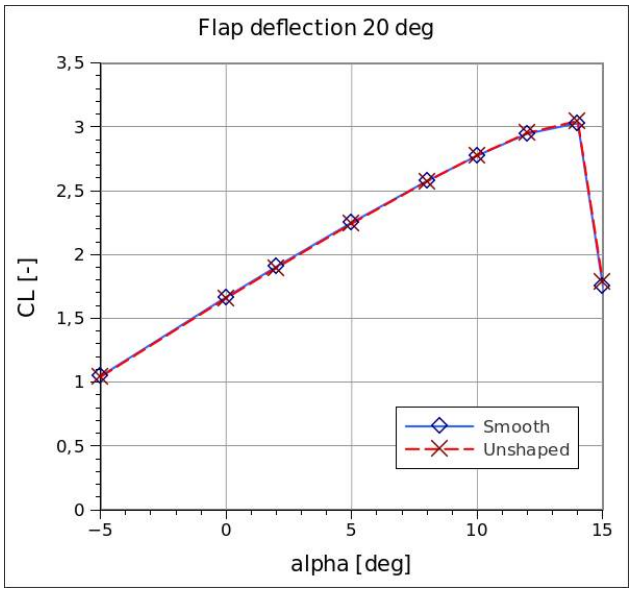

Fig. 13. Lift Curves for Take-off Configuration (CFD Results)

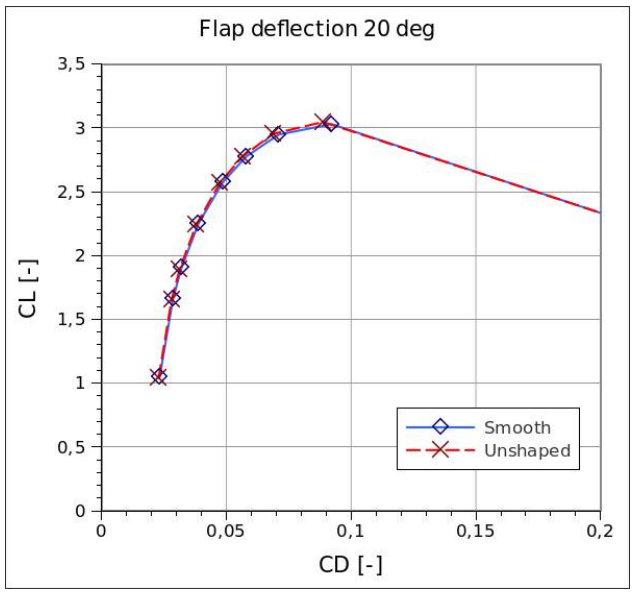

Fig. 14. Polar Curves for Take-off Configuration (CFD results)

The CFD flowfield visualization results are very close to the experimental results, they similarly show that the vortices in the cove are formed in such manner, that the effective path of the passing stream stays nearly identical for both geometries (see Fig.15. to Fig. 17.).

Due to closeness of the CFD and experimental results, it is possible to use the CFD results to investigate the areas that are not covered by PIV. Namely the large open gap of the cove of the unshaped geometry where the PIV was not usable due to pronounced shadows that prevent from taking the images. The CFD computations show distinct vortex system created in the open gap of the unshaped geometry, this system is of low intensity, nevertheless it consumes certain power to keep in, which explains slightly higher drag of this geometry.

The vortex strength was computed for the corresponding areas for both the PIV and CFD results. For the landing configuration with alpha of 10 deg the dimensionless vortex strength is -0.136 from PIV results and -0.113 from CFD results.

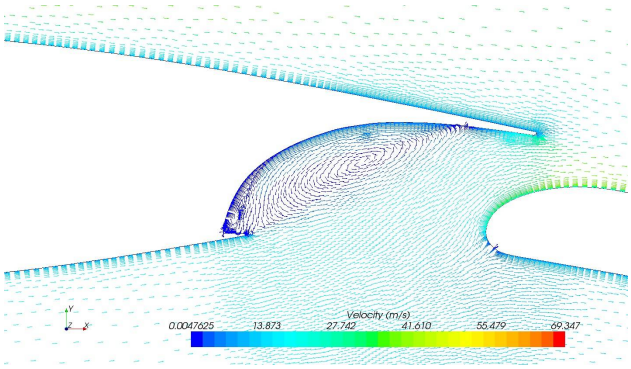

Fig. 15. Velocity Distribution, Take-off Configuration, alpha 10 deg (CFD results)

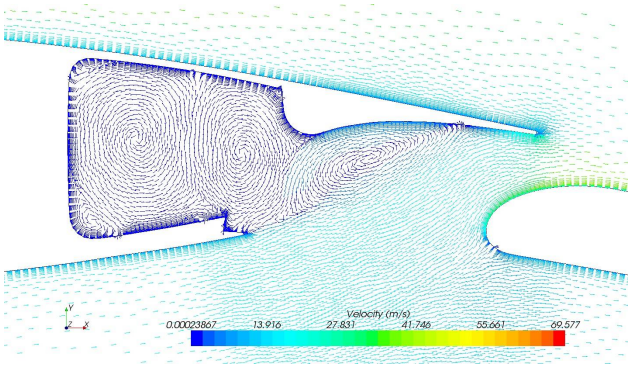

Fig. 16. Velocity Distribution, Take-off Configuration, alpha 10 deg (CFD results)

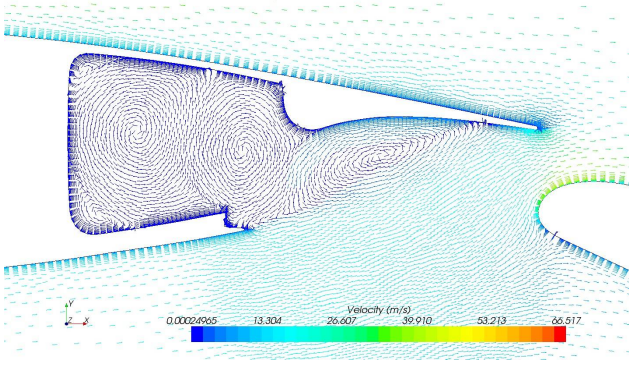

Fig. 17. Velocity Distribution, Landing Configuration, alpha 10 deg (CFD results)

7 Conclusions

The main conclusion is that the form of the trailing edge of the main airfoil is of moderate importance regarding the effective cross section of the gap between the main airfoil and the Fowler flap. The principal vortex forming the gap shape is similar in the both cases tested, the vortex in simply open trailing part of the main airfoil fills the space in such manner that the effective gap between the main airfoil and the flap is similar like with carefully shaped trailing edge. As consequence, the efficiencies of the flap are very similar and the increments of c_L nearly identical.

The large but low-intensity vortex system in the open gap consumes certain power so the total airfoil drag is slightly higher at identical lift. But the open access to the spar and the possibility to use available free space can be more beneficial from the global point of view of aircraft designer.

References

[1] Cebeci, T., Besnard, E., Chen, H. H., Calculation of Multielement Airfoil Flows, including Flap Wells, AIAA Paper 96-0056

[2] Savory, E., Toy, N., Tahouri, B., Dalley, S., Flow regimes in the cove regions between a slat and wing and between a wing and flap of a multielement airfoil, Experimental Thermal and Fluid Science, Volume 5, Issue 3, May 1992, Pages 307-316

[3] Maddah, S.R., Bruun, H. H., Experimental Investigation of Flowfield over a Multi-element Aerofoil and Comparison with Computational Prediction, ICAS 2000 Congress Proceedings 297.1

[4] Nakayama, AIAA Journal Vol. 28 (1990), No. 1, pp. 14 – 21

[5] Wentz, W. H., Jr.; Ostowari, C., Additional flow field studies of the GA(W)-1 airfoil with 30-percent chord Fowler flap including slot-gap variations and cove shape modifications, NASA-CR-3687, NASA 1983

[6] Pátek, Z., Zabloudil, M., Pressure Distribution Development on an Airfoil with a Fowler Flap, RRDPAE Proceedings Volume 2008, Brno, Czech Republic, 2008, ISSN 1425-2104

Copyright Statement